T. Wakabayashi
e-mail: twakaba@osakagas.co.jp

S. Ito
e-mail: ito@osakagas.co.jp

S. Koga
e-mail: s-koga@osakagas.co.jp

M. Ippommatsu
e-mail: m-ippommatsu@osakagas.co.jp

K. Moriya
e-mail: moriya@osakagas.co.jp

Osaka Gas Co., Ltd.,
6-19-9, Torishima,
Konohana-ku,
Osaka 554-0051, Japan

K. Shimodaira
e-mail: simo@nal.go.jp

Y. Kurosawa
e-mail: kuro@nal.go.jp

K. Suzuki
e-mail: suzukazu@nal.go.jp

National Aerospace Laboratory,
7-44-1 Jindaiji-higashi,
Chofu, Tokyo 182-8522, Japan

Performance of a Dry Low-NO_x Gas Turbine Combustor Designed With a New Fuel Supply Concept

This paper describes the performance of a dry low-NO_x gas turbine combustor designed with a new fuel supply concept. This concept uses automatic fuel distribution achieved by an interaction between the fuel jet and the airflow. At high loads, most of the fuel is supplied to the lean premixed combustion region for low-NO_x, while at low loads, it is supplied to the pilot combustion region for stable combustion. A numerical simulation was carried out to estimate the equivalence ratio in the fuel supply unit. Next, through the pressurized combustion experiments on the combustor with this fuel supply unit using natural gas as fuel, it was confirmed that NO_x emissions were reduced and stable combustion was achieved over a wide equivalence ratio range. [DOI: 10.1115/1.1473154]

Introduction

The reduction of NO_x emissions from stationary gas turbines is necessary to meet the increasingly stringent emissions standards imposed by regulatory agencies worldwide. Current practices involve the injection of water or steam and the use of selective catalytic reduction. These abatement methods have specific limitations and problems, including high installation and operating costs and the requirement of large installation space.

Lean premixed combustion is an effective way to reduce these emissions, and development programs of dry low-NO_x combustors using lean premixed combustion concepts are being actively conducted by several gas turbine manufactures ([1]). However, the stable operating range becomes narrow when this method is applied without any supplementary control. Many techniques have been developed to solve this problem: parallel fuel staging ([2–5]), series fuel staging ([6]), and variable geometry systems, such as, inlet guide vane modulation ([7]), air bleed ([8]), and swirler inlet air control ([7,9]).

However, parallel or series fuel staging requires individual fuel supply devices for each group of burners, and variable geometry systems have problems in reliability and durability, since movable parts are needed in the high-pressure high-temperature gas stream. Furthermore, neither can respond smoothly to rapid load changes.

In order to solve these problems, a new fuel supply concept has been proposed. This concept uses automatic fuel distribution achieved by an interaction between the fuel jet and the airflow. A schematic diagram of the new concept is shown in Fig. 1. A fuel supply unit is placed at the forward part of a combustor. This unit has an outer main region for lean premixed combustion and an inner pilot region for stable combustion. The air velocity in the main region is higher than in the pilot region. Fuel is supplied through only one line. A fuel passage hole (B) is located at the outer position of a fuel injection nozzle (A). There is a gap between these parts, and combustion air flows through this gap.

At high loads, the fuel jet has so much momentum that it penetrates the airflow through the gap. More fuel is supplied to the main region than to the pilot region and consequently the rate of lean premixed combustion increases. At low loads, the fuel jet has low momentum. More fuel is supplied to the pilot region than to the main region and consequently the combustion becomes stable.

As the fuel distribution ratio between the main and the pilot region changes automatically when the load of the gas turbine is changed, this combustion system offers good response for rapid load changes.

Design of Fuel Supply Unit by Numerical Simulation

Figure 2 shows a cross section of the prototype combustor and the test rig. This combustor is one of six can-annular-type combustors (4000 kW class). This combustor has a fuel supply unit, a liner (ID: 142.3 mm) and a transition piece.

The details of the fuel supply unit are shown in Fig. 3. The unit has an outer main region for lean premixed combustion and an inner pilot region for stable combustion. The air velocity in the main region is higher than in the pilot region.

A fuel passage hole (B: 2.6 mm dia.) is located at the outer position of the fuel injection nozzle (A: 1.6 mm dia.). There is a

Contributed by the International Gas Turbine Institute (IGTI) of THE AMERICAN SOCIETY OF MECHANICAL ENGINEERS for publication in the ASME JOURNAL OF ENGINEERING FOR GAS TURBINES AND POWER. Paper presented at the International Gas Turbine and Aeroengine Congress and Exhibition, New Orleans, LA, June 4–7, 2001; Paper 01-GT-050. Manuscript received by IGTI, December 2000, final revision, March 2001. Associate Editor: R. Natole.

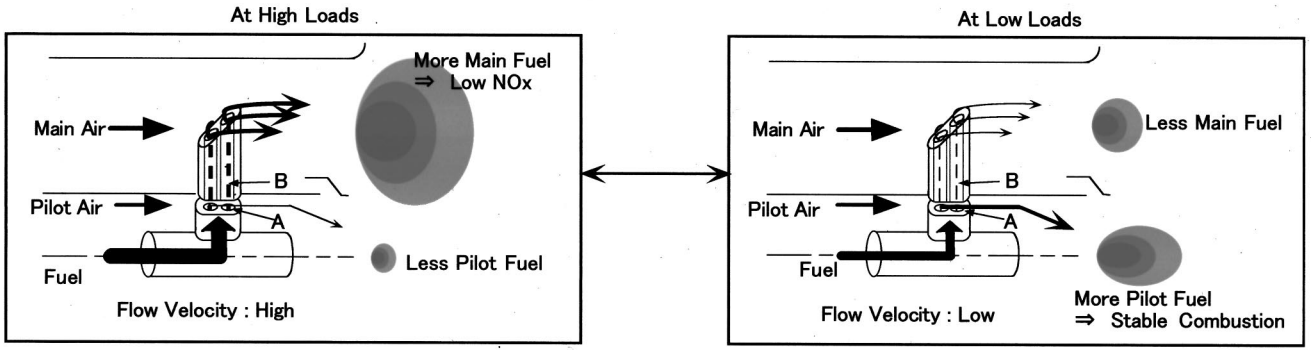

Fig. 1 New Fuel supply concept

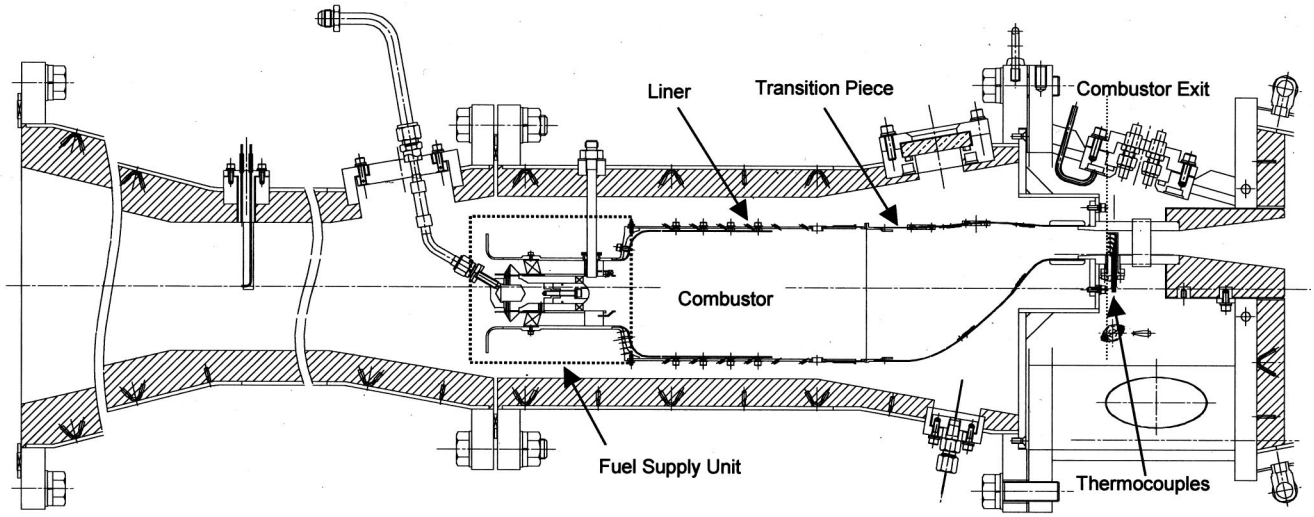

Fig. 2 Cross section of the prototype combustor and the test rig

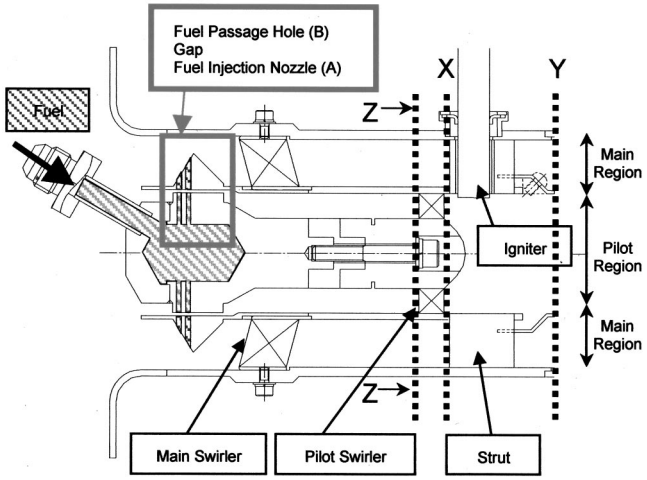

Fig. 3 Details of the fuel supply unit

gap (1.2 mm) between these parts, and the pilot air for combustion flows through this gap. Two sets of this device were positioned axially at each of eight locations arranged in a circle.

The temperature of the inlet air is 623 K and the combustor air velocity at the liner is 24 m/s.

First, in order to verify that more fuel is distributed to the main region at high loads and to the pilot region at low loads, the equivalence ratio in the fuel supply unit shown in Fig. 3 was calculated by numerical simulation in a noncombusting state. The standard $k-\varepsilon$ model was used to take account of turbulence. A multiblock grid system was adopted to make the mesh configuration sufficiently fine around the zone adjacent to the fuel jet, in order to precisely analyze the interaction between the free stream fluid and the fuel jets. All significant parts were three dimensionally modeled, including swirlers, which would be relative to the pressure resistance and fuel mixing, and important in prediction of the flow rates in the main and pilot region as well as the profile of the fuel concentrations.

The equivalence ratio patterns in the fuel supply unit and at the exit of the fuel supply unit (dotted line Y) were calculated at six different total equivalence ratios (ϕ_t), i.e., 0.05, 0.10, 0.15, 0.20, 0.25, and 0.30 (see Fig. 4). Figure 4 indicates that more fuel is distributed to the main region at high loads and to the pilot at low loads. Further at high load ($\phi_t=0.3$) the equivalence ratio pattern at the exit of the fuel supply unit is very uniform for the reduction of NO_x, and at low load ($\phi_t=0.2$) less fuel is distributed to the tip side in the main region for the improvement of combustion efficiency.

Figure 5 shows the dependence of the average equivalence ratio in the main region at the dotted line X (ϕ_m) on the total equivalence ratio (ϕ_t) by numerical simulation. In the equivalence range of 0.00 to 0.15, ϕ_m is estimated to be almost zero. Further, it is estimated that above 0.15, the higher ϕ_t becomes, the higher ϕ_m becomes linearly. These results support the new fuel supply concept shown in Fig. 1.

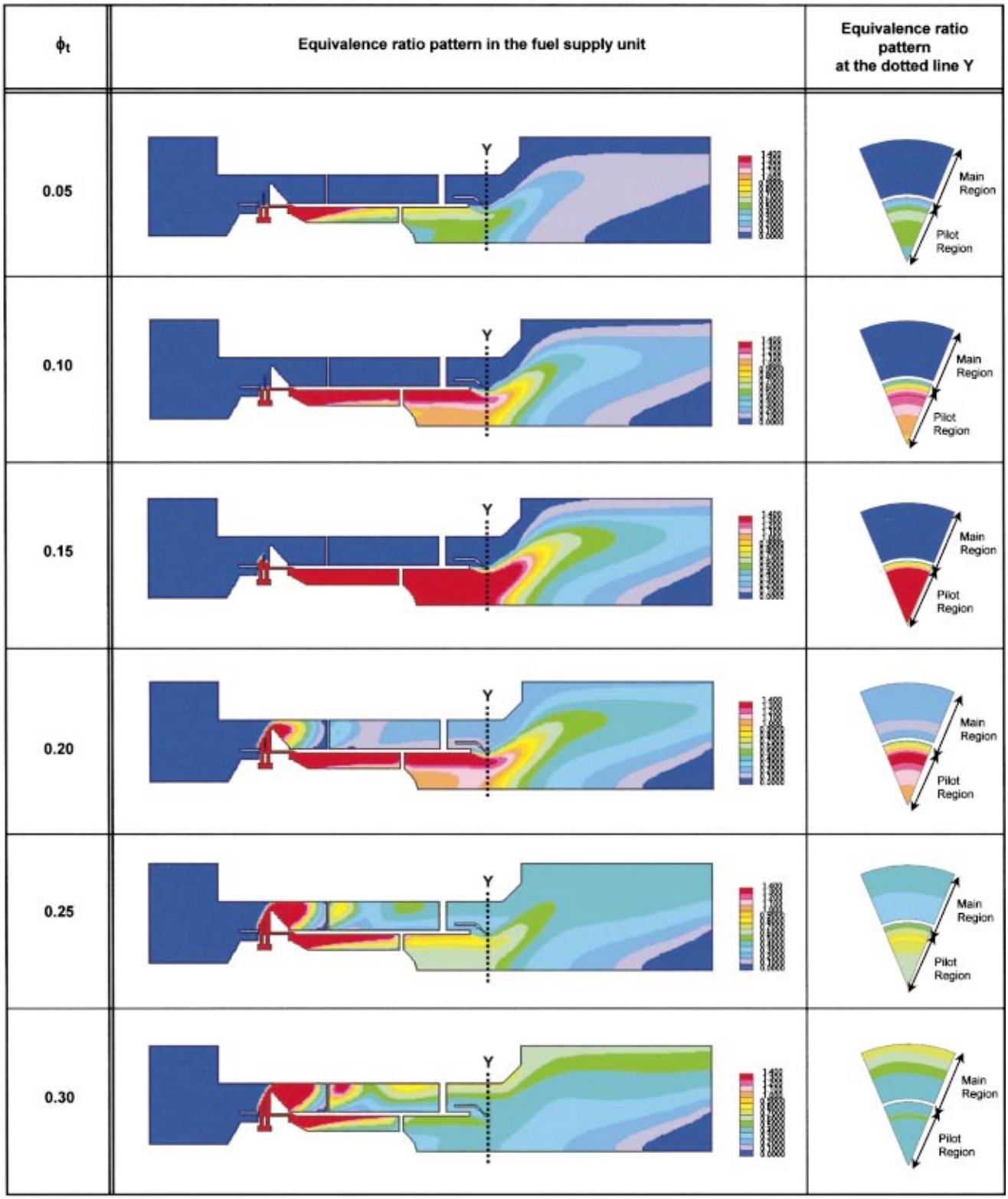

Fig. 4 Equivalence ratio pattern in the fuel supply unit by numerical simulation

Therefore, we decided to measure the pressurized combustion performance on the combustor with the fuel supply unit shown in Fig. 3.

Experimental Apparatus

The pressurized combustion test facility is shown in Fig. 6. The temperature of the inlet air was 623 K, and the combustor air velocity at the liner was 24 m/s. Combustion tests were conducted at four different compressor discharge pressures (CDP), i.e., 0.15, 0.40, 0.60, and 0.80 MPa. Natural gas (methane: 88%, ethane: 6%, propane: 4% and butane: 2%) was used as fuel.

The NO_x, O_2, CO, CO_2, and THC concentrations were measured in the exhaust gas. A water-cooled sampling probe was mounted at a location about 1 m downstream from the combustor

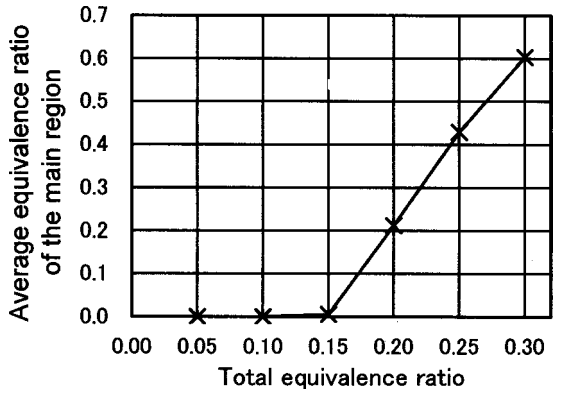

Fig. 5 Average equivalence ratio of the main region by numerical simulation

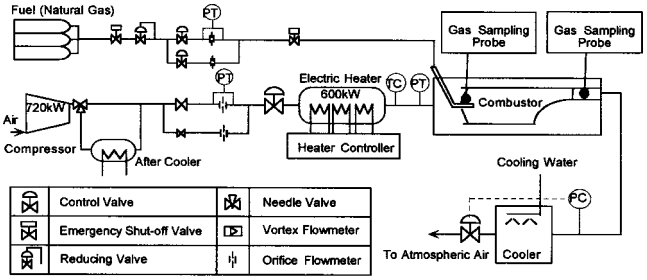

Fig. 6 Pressurized combustion test facility

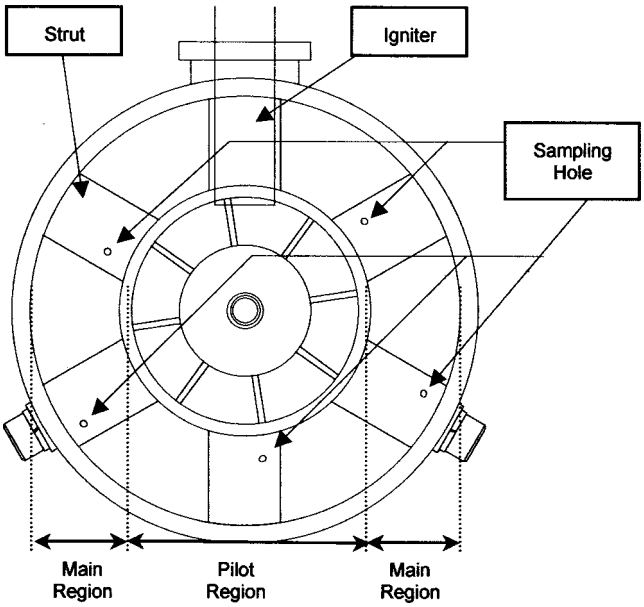

Fig. 7 Cross section (Z-Z) of fuel supply unit (see Fig. 3)

exit. This probe was designed to mix equal amounts of exhaust gas sampled from seven holes, each measuring 1.0 mm in diameter. The combustion efficiency and the total equivalence ratio (ϕ_t) were calculated from the measured exhaust gas compositions.

To evaluate experimentally whether the fuel distribution shown in Fig. 1 was actually achieved, THC and O_2 concentrations in the main mixture at the fuel supply unit were also measured. There were six structures, termed struts, in the main region (see Figs. 3 and 7). Sampling holes (1.3 mm dia.) were in five of the struts excluding the one that houses the igniter. The sampling holes were dispersed in the tip side and hub side of the main region. Equal amounts of the sampling gas from five holes were mixed and sent to the gas analyzer. The main equivalence ratio (ϕ_m) was calculated from the measured gas compositions.

The average temperature of the exhaust gas at the combustor exit, called BOT, was measured by 50 thermocouples (R-type, inconel sheath, 1.6 mm dia., see Fig. 2).

Experimental Results and Discussion

First, it was confirmed that ignition was possible and stable combustion was achieved in all loads even with only one fuel line in this prototype combustor.

Figure 8 shows the relation between the average equivalence ratio in the main region (ϕ_m) and the total equivalence ratio (ϕ_t). The numerical prediction shows good agreement with the experimental results. The CDP difference does not affect this relation. In the equivalence ratio range of 0.00 to 0.15, ϕ_m is almost zero. Above 0.15, the higher ϕ_t becomes, the higher ϕ_m becomes linearly. The reason for this is as follows. The fuel jet in the equivalence ratio range of 0.00 to 0.15 does not have enough momentum to penetrate the gap. At the equivalence ratio of 0.15, the fuel jet is able to penetrate the gap and a part of the fuel starts being supplied to the main region. Above 0.15, the fuel jet has enough momentum to penetrate the gap, and the higher ϕ_t becomes, the more momentum the jet has.

Figure 9 shows the relation between NO_x emissions (at 0% O_2) and the total equivalence ratio (ϕ_t). The CDP difference affects this relation intensely. The higher the CDP becomes, the higher NO_x emissions become. Figure 10 shows the relation between

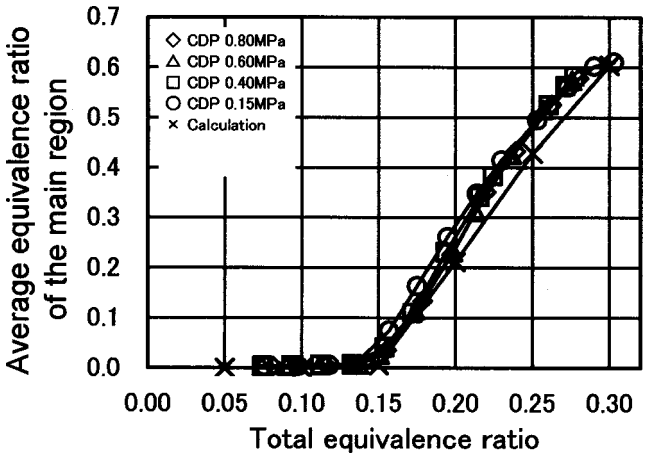

Fig. 8 Average equivalence ratio of the main region

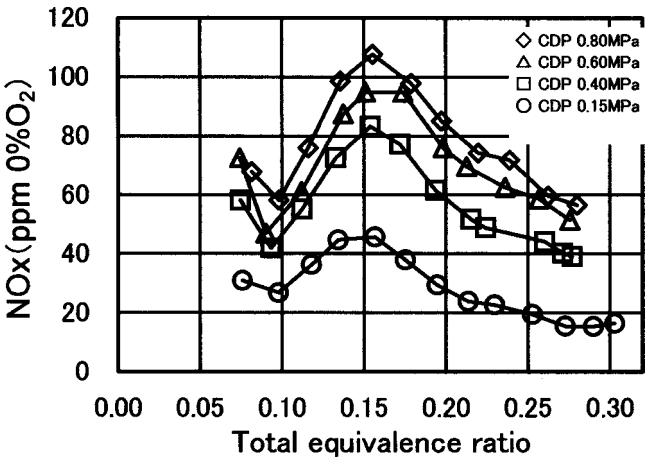

Fig. 9 NO_x emissions (at 0% O_2)

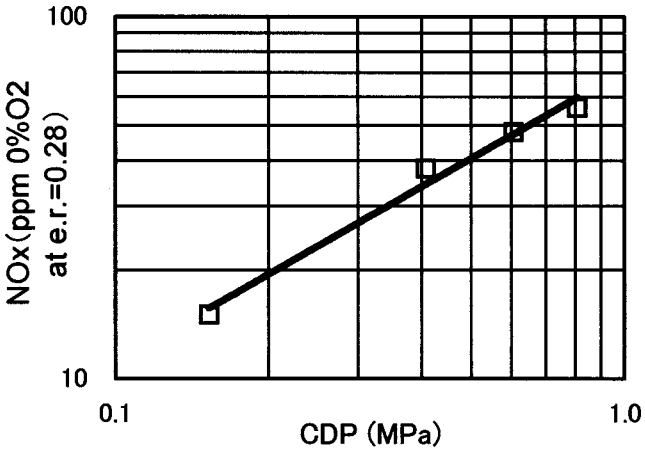

Fig. 10 Dependence of NO_x emissions on CDP

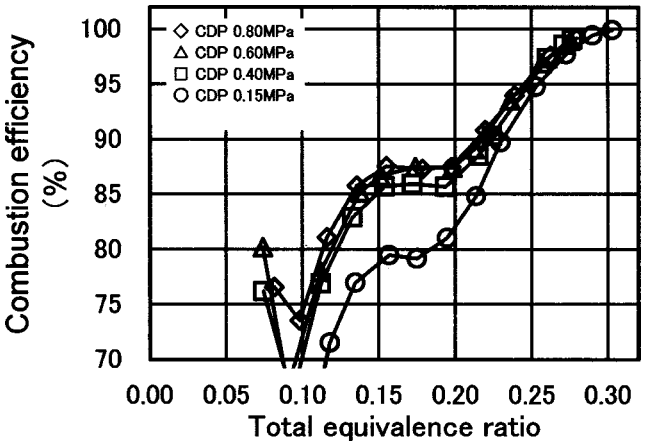

Fig. 11 Combustion efficiency

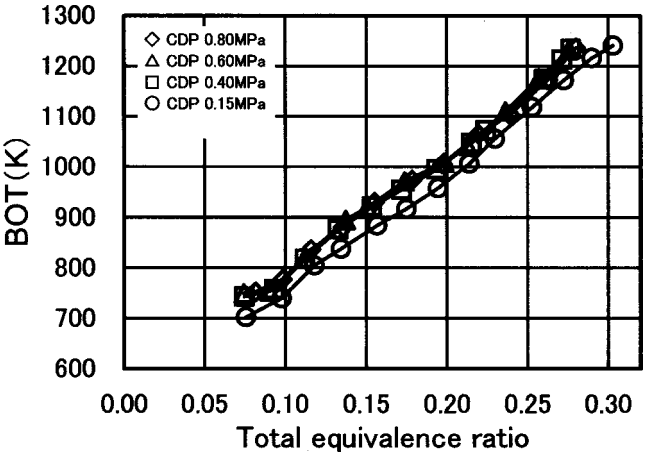

Fig. 12 Average temperature of exhaust gas at the exit of the combustor

NO_x emissions (at 0% O_2) and CDP at an equivalence ratio of about 0.28. NO_x emissions are proportional to the CDP to the power of about 0.81 in this prototype combustor.

NO_x emissions increase up to an equivalence ratio of 0.15 and decrease above 0.15. This behavior is the same under all CDP values. The reason for this performance is estimated as follows, using the results of the numerical simulation and the combustion experiment above (see Figs. 4 and 8). Under any CDP value, in the equivalence ratio range of 0.00 to 0.15, ϕ_m is almost zero. But above 0.15, the higher ϕ_t becomes, the higher ϕ_m becomes linearly. Further, the uniform equivalence ratio pattern at the dotted line Y makes it possible to reduce NO_x emissions at high loads. It was confirmed that NO_x emissions (at 0% O_2) were below 60 ppm under the condition that CDP was 0.80 MPa and ϕ_t was about 0.28.

Figure 11 shows the relation between the combustion efficiency and the total equivalence ratio (ϕ_t). The CDP difference affects this relation moderately. At the same equivalence ratio, the higher the CDP becomes, the higher the combustion efficiency becomes. The tendency of the relation is the same under any CDP value. In the equivalence ratio range from 0.20 to 0.30, the lower the combustion efficiency becomes, the lower ϕ_t becomes. However, even if ϕ_t decreases in the equivalence ratio of 0.15 to 0.20, the combustion efficiency does not decrease. The reason for this is assumed to be that in this equivalence range, the fuel distribution ratio to the pilot increases intensely when ϕ_t decreases. Therefore stable combustion is achieved at low loads and the combustion efficiency does not decrease.

Figure 12 shows the relation between BOT and the total equivalence ratio (ϕ_t). The CDP difference affects this relation moderately. When CDP is 0.80 MPa and the equivalent ratio is 0.28, the BOT is about 1240 K.

Conclusion

In order to obtain low-NO_x characteristics over a wide operating range without any supplementary control, a new fuel supply concept was proposed in this paper. This concept uses automatic fuel distribution achieved by an interaction between the fuel jet and the airflow. At high loads, most of the fuel is supplied to the lean premixed combustion region to reduce NO_x emissions, while at low loads, it is supplied to the pilot combustion region to stabilize combustion.

First, the fuel distribution of a prototype combustor was calculated by numerical simulation, and it was confirmed that the results of the numerical simulation support the new fuel supply concept described above.

Next, through pressurized combustion experiments on the combustor with this fuel supply unit using natural gas as fuel, it was confirmed that NO_x emissions were reduced (under 60 ppm at 0% O_2 $\phi_t = 0.28$) and stable combustion was achieved over a wide equivalence ratio range.

This simple structure makes it possible to reduce NO_x emissions without additional apparatus, helping to lower the cost of equipment and to improve the reliability and durability of combustors.

References

[1] Solt, J. C., and Tuzson, J., 1993, "Status of Low NO_x Combustor Development," ASME Paper No. 93-GT-270.

[2] Aigner, M., and Muller, G., 1993, "Second-Generation Low-Emission Combustors for ABB Gas Turbines: Field Measurements with GT11N-EV," ASME J. Eng. Gas Turbines Power, **115**, pp. 533–536.

[3] Kitajima, J., Kimura, T., Sasaki, T., Okuto, A., Kajita, S., Ohga, S., and Ogata, M., "Development of a Second Generation Dry Low NO_x Combustor for 1.5MW Gas Turbine," ASME Paper No. 95-GT-255.

[4] Ishii, J., 1999, "The Next Generation High-Efficiency Combined-Cycle Power Plants which used 1500C-class Steam Cooled Gas Turbine," Journal of the Gas Turbine Society of Japan, **27**(3), pp. 161–165.

[5] Akita, E., and Nishida, M., 1999, "Development and Verificational Operation of 1500C Class Next Generation High Efficient G series Gas Turbine," Journal of the Gas Turbine Society of Japan, **27**(3), pp. 138–145.

[6] Sato, H., Amano, T., Iiyama, Y., Mori, M., and Nakamura, T., 1999, "Development of a Three-Staged Low Emissions Combustor for Industrial Small-Size Gas Turbines," ASME Paper No. 99-GT-236.

[7] Smith, K. O., 1992, "Engine Testing of a Prototype Low NO_x Gas Turbine Combustor," ASME Paper No. 92-GT-116.

[8] Etherdge, C. J., 1994, "Mars SoLoNO_x-Lean Premix Combustion Technology in Production," ASME Paper No. 94-GT-255.

[9] Smith, K. O., Holsapple, A. C., Mak, H. K., and Watkins, L., 1991, "Development of a Natural Gas Fired, Ultra-Low NO_x Can Combustor for 800 kW Gas Turbine Engines," ASME Paper No. 91-GT-303.